Infinite volume and continuum limits for the gluon propagator in $3d$ $SU(2)$ lattice gauge theory

V. G. Bornyakov

Institute for High Energy Physics, 142281 Protvino, Russia
and Institute of Theoretical and Experimental Physics, 117259 Moscow, Russia

V. K. Mitrjushkin

Joint Institute for Nuclear Research, 141980 Dubna, Russia
and Institute of Theoretical and Experimental Physics, 117259 Moscow, Russia

R. N. Rogalyov

Institute for High Energy Physics, 142281 Protvino, Russia
(Received 6 June 2013; revised manuscript received 18 December 2013; published 17 March 2014)

We study the Landau gauge gluon propagator $D(p)$ in the three-dimensional $SU(2)$ lattice gauge theory. We show that in the infinite-volume limit the expectation values over the Gribov region Ω are *different* (in the infrared) from that calculated in the fundamental modular region Γ. Also we show that this conclusion does *not* change when spacing a tends to zero.

DOI: 10.1103/PhysRevD.89.054504 PACS numbers: 11.15.Ha, 12.38.Aw, 12.38.Gc

I. INTRODUCTION

There are various scenarios of confinement based on infrared behavior of the gauge-dependent propagators. For example, in the Gribov-Zwanziger (GZ) confinement scenario [1,2] the Landau gauge gluon propagator $D(p)$ at infinite volume is expected to vanish in the infrared limit $p \to 0$. At the same time, a refined Gribov-Zwanziger (RGZ) scenario [3–5] allows a finite nonzero value of $D(0)$. The nonperturbative lattice calculations are necessary to check the validity of each scenario as well as to check the results obtained by analytical methods, e.g., the (truncated) Dyson-Schwinger equations (DSE) approach. The DSE scaling solution predicts that the propagator tends to zero in the zero-momentum limit [6,7] in accordance with the GZ scenario. Another decoupling solution [8–11] allows a finite nonzero value of $D(0)$ in conformity with the RGZ scenario.

The three-dimensional $SU(2)$ theory can serve as a useful test ground to verify these predictions. It is also of interest for the studies of the high-temperature limit of the four-dimensional theory. Last year the three-dimensional theory was numerically studied in a number of papers [12–18]. It was shown that the propagator has a maximum at momenta about 350–400 MeV and that zero momentum propagator $D(0)$ does not tend to zero in the infinite-volume limit [14,18].

The Gribov copy problem still remains one of the main difficulties in computation of the gauge-dependent objects (for a recent review see [19], for the three-dimensional case see, e.g., [18] and references therein).

The manifold consisting of Gribov copies providing local maxima of the gauge-fixing functional and a semi-positive Faddeev-Popov operator is termed the *"Gribov region"* Ω, while that of the global maxima is termed the *"fundamental modular region"* $\Gamma \subset \Omega$ [20]. Our gauge-fixing procedure is aimed to approach Γ.

In paper [21] it was claimed that although there are Gribov copies inside the Gribov region Ω, they have no influence on expectation values in the thermodynamic limit, i.e., for any gauge noninvariant observable O,

$$\langle O \rangle_\Omega = \langle O \rangle_\Gamma. \tag{1}$$

In our recent paper [18] we attempted to check this statement. We calculated gluon propagators $D(p)$ on different lattices (for $p = 0$ as well as for $p \neq 0$) and then extrapolated the values of D in the thermodynamic limit. It was shown that in the thermodynamic limit $L \to \infty$, Gribov copies have a significant effect on the value of $D(0)$.

Most of our calculations in [18] were performed at $\beta = 4.24$ ($a = 0.17$ fm). The main goals of this paper are (a) to find confirmation of our observations made in [18] employing different (larger) values of β and (b) to draw some definite conclusions about the continuum limit of the theory.

In Sec. II we introduce the quantities to be computed and give some details of our simulations. In Sec. III we present our numerical results. Conclusions are drawn in Sec. IV.

II. MAIN DEFINITIONS AND DETAILS OF THE SIMULATION

We consider three-dimensional cubic lattice L^3 with spacing a. To generate Monte Carlo ensembles of thermalized configurations, we use the standard Wilson action,

$$S = \beta \sum_{x,\mu>\nu} \left[1 - \frac{1}{2} \operatorname{Tr} \left(U_{x\mu} U_{x+\hat{\mu}a;\nu} U^{\dagger}_{x+\hat{\nu}a;\mu} U^{\dagger}_{x\nu} \right) \right], \quad (2)$$

where $\beta = 4/g_B^2 a$, $\hat{\mu}$ is a vector of unit length along the μth coordinate axis, and g_B denotes dimensionful bare coupling. $U_{x\mu} \in SU(2)$ are the link variables that transform under local gauge transformations g_x as follows:

$$U_{x\mu} \overset{g}{\mapsto} U^g_{x\mu} = g^{\dagger}_x U_{x\mu} g_{x+\hat{\mu}a}, \qquad g_x \in SU(2). \quad (3)$$

In Table I we provide the full information about the field ensembles used in this investigation. The scale is set in accordance with [22], where string tension is $\sqrt{\sigma} = 440$ MeV.

We study the gluon propagator

$$D^{\rm bc}_{\mu\nu}(q) = \frac{a^3}{L^3} \sum_{x,y} \exp\left(iqx + \frac{ia}{2} q(\hat{\mu} - \hat{\nu}) \right) \times \left\langle A^b_{\mu}\left(x + y + \frac{\hat{\mu}a}{2} \right) A^c_{\nu}\left(y + \frac{\hat{\nu}a}{2} \right) \right\rangle, \quad (4)$$

where the vector potentials $A^a_{\mu}(x)$ are defined as follows [23],

$$A_{\mu}\left(x + \frac{\hat{\mu}a}{2} \right) \equiv \sum_{b=1}^{3} A^b_{\mu} \sigma^b = \frac{i}{a g_B} (U_{x\mu} - U^{\dagger}_{x\mu}), \quad (5)$$

TABLE I. Values of lattice size, L, number of measurements $n_{\rm meas}$, and number of gauge copies $n_{\rm copy}$ used throughout this paper.

$\beta = 7.09$ ($a = 0.094$ fm)				
L	$n_{\rm meas}$	$n_{\rm copy}$	aL [fm]	$p_{\rm min}$ [GeV]
36	2000	160	3.38	0.365
42	2800	160	3.96	0.313
48	900	160	4.51	0.274
56	900	160	5.26	0.234
64	1200	160	6.02	0.205
78	900	280	7.33	0.168
92	1000	280	8.65	0.143
108	300	280	10.18	0.122

$\beta = 10.21$ ($a = 0.063$ fm)				
L	$n_{\rm meas}$	$n_{\rm copy}$	aL [fm]	$p_{\rm min}$ [GeV]
36	2800	160	2.27	0.546
42	1600	160	2.65	0.467
48	2000	160	3.02	0.408
56	1400	160	3.53	0.350
64	1200	160	4.03	0.306
76	1100	280	4.80	0.258
96	1200	280	6.05	0.204

and the momenta q_{μ} take the values $q_{\mu} = 2\pi n_{\mu}/aL$, where n_{μ} runs over integers in the range $-L/2 \le n_{\mu} < L/2$. The gluon propagator can be represented in the form

$$D^{\rm bc}_{\mu\nu}(q) = \begin{cases} \delta^{\rm bc} \delta_{\mu\nu} D(0), & p = 0, \\ \delta^{\rm bc} \left(\delta_{\mu\nu} - \frac{p_{\mu} p_{\nu}}{p^2} \right) D(p), & p \neq 0, \end{cases}$$

where $p_{\mu} = \frac{2}{a} \sin \frac{q_{\mu} a}{2}$ and $p^2 = \sum_{\mu=1}^{3} p^2_{\mu}$. For $p \neq 0$ one arrives at

$$D(p) = \frac{1}{6} \frac{1}{(La)^3} \sum_{\mu=1}^{3} \sum_{b=1}^{3} \langle \tilde{A}^b_{\mu}(q) \tilde{A}^b_{\mu}(-q) \rangle, \quad (6)$$

where

$$\tilde{A}^b_{\mu}(q) = a^3 \sum_x A^b_{\mu}\left(x + \frac{\hat{\mu}a}{2} \right) \exp\left(iq\left(x + \frac{\hat{\mu}a}{2} \right) \right), \quad (7)$$

and the zero-momentum propagator has the form

$$D(0) = \frac{1}{9} \frac{1}{(La)^3} \sum_{\mu=1}^{3} \sum_{b=1}^{3} \langle \tilde{A}^b_{\mu}(0) \tilde{A}^b_{\mu}(0) \rangle. \quad (8)$$

In what follows we use the gluon propagator $D(p)$ normalized at $\mu = 2.5$ GeV, so that $p^2 D(p) = 1$ for $p^2 = \mu^2$.

We employ the usual choice of the Landau gauge condition on the lattice [23],

$$(\partial A)(x) = \frac{1}{a} \sum_{\mu=1}^{3} \left(A_{\mu}\left(x + \frac{\hat{\mu}a}{2} \right) - A_{\mu}\left(x - \frac{\hat{\mu}a}{2} \right) \right) = 0, \quad (9)$$

which is equivalent to finding a local extremum of the gauge-fixing functional,

$$F_U[g] = \frac{1}{3L^3} \sum_{x\mu} \frac{1}{2} \operatorname{Tr} U^g_{x\mu}, \quad (10)$$

with respect to gauge transformations g_x.

To fix the gauge we choose for every gauge orbit a representative from Γ [20], i.e., the absolute maximum of the gauge-fixing functional $F_U[g]$. This choice is well consistent with a nonperturbative Parrinello-Jona-Lasinio-Zwanziger gauge-fixing approach [24,25] which presumes that a unique representative of the gauge orbit needs the global extremum of the chosen gauge- fixing functional. Also in the case of pure gauge $U(1)$ theory in the Coulomb phase some of the gauge copies produce a photon propagator with a decay behavior inconsistent with the expected zero mass behavior [26–28]. However, the choice of the global extremum permits to obtain the massless photon propagator.

For practical purposes, it is sufficient to approach the global maximum close enough so that the systematic errors due to nonideal gauge fixing (because of, e.g., Gribov copy effects) are of the same magnitude as statistical errors. This strategy was checked in a number of papers on four-dimensional and three-dimensional theory studies for both $SU(2)$ [18,29–33] and $SU(3)$ [34,35] gauge groups. For recent alternative attempts, see [36–38].

The gluon propagator in the deep infrared region can be reliably evaluated only when the effects of Gribov copies are properly taken into account. The gauge-fixing procedure that we use was already successfully employed in the four-dimensional theory at both zero [31,32] and nonzero [33,34] temperature. There are three main ingredients in this procedure: the powerful simulated annealing algorithm, which proved to be efficient in solving various optimization problems; the flip transformation of gauge fields, which was used to decrease both the Gribov-copy and finite-volume effects [31–33]; and the simulation of a large number of gauge copies for each flip sector in order to further decrease the effects of Gribov copies.

All details of our gauge-fixing procedure can be found, e.g., in [18]. For the reader's convenience, we will describe it shortly here.

First, we extend the gauge group by the transformations (also referred to as Z_2 flips) defined as follows,

$$f_\nu(U_{x,\mu}) = \begin{cases} -U_{x,\mu} & \text{if } \mu=\nu \quad \text{and} \quad x_\mu = a, \\ U_{x,\mu} & \text{otherwise} \end{cases}$$

which are the generators of the Z_2^3 group leaving the action (2) invariant. Such flips are equivalent to nonperiodic gauge transformations. A Polyakov loop directed along the transformed links and averaged over the two-dimensional plane changes its sign. Therefore, the flip operations combine the 2^3 distinct gauge orbits (or Polyakov loop sectors) of strictly periodic gauge transformations into one larger gauge orbit.

We use the simulated annealing algorithm, which was found to be computationally more efficient than the use of the standard overrelaxation (OR) only [30,39,40]. The simulated annealing algorithm generates gauge transformations g_x by MC iterations with a statistical weight proportional to $\exp(3VF_U[g]/T)$. The "temperature" T is an auxiliary parameter which is gradually decreased in order to maximize the gauge functional $F_U[g]$. In the beginning, T has to be chosen sufficiently large in order to allow traversing the configuration space of g_x fields in large steps. T is decreased with equal step size. The final temperature is fixed such that during the consecutively applied OR algorithm, the violation of the transversality condition

$$\frac{g_B a^2}{2} \max_{x,c} |(\partial A^c)(x)| < \epsilon \tag{11}$$

decreases in a more or less monotonous manner for the majority of gauge-fixing trials until the condition (11) becomes satisfied with $\epsilon = 10^{-7}$.

To finalize the gauge-fixing procedure, we apply the OR algorithm with the standard Los Alamos–type overrelaxation. In what follows, this method is labeled "FSA" (flipped simulated annealing). To demonstrate the effect of flip sectors, we also use the gauge-fixing procedure without flips, labeled "SA" (simulated annealing) (for details see [18]).

We then take the best copy (bc) out of many gauge-fixed copies obtained for the given gauge field configuration, i.e., a copy with the maximal value of the lattice gauge-fixing functional $F_U[g]$ as a best estimator of the *global* extremum of this functional.

To demonstrate the effect of Gribov copies, we also consider the gauge obtained by a random choice of a copy within the first Gribov horizon, the first copy (fc); i.e., we take the first copy obtained by our gauge-fixing procedure. It is instructive also to compare bc and fc propagators with the worst copy (wc) propagators, which correspond to the choice of the gauge copy with minimal value of the gauge-fixing functional.

III. NUMERICAL RESULTS

To estimate the infinite-volume limits $L \to \infty$ of the zero-momentum gluon propagators $D(0;L)$ we apply a few different fit-formulas :

(A) $c_1 + c_2/L$;
(B) $c_1 + c_2/L + c_3/L^2$;
(C) $c_1 + c_2/L^\gamma$;
(D) c_2/L^γ,

where c_1, c_2, c_3 and γ are fit-parameters.

Calculations on rather large lattices (up to $L = 320$) and $\beta = 3.0$ showed [14] that the fit-formula (A) works well for large values of L (at least, in the minimal Landau gauge) with nonvanishing value of $D(0,L)$ in the thermodynamic limit (i.e., $c_1 \neq 0$). On the contrary, the fit-formula (D) used in [16] (for comparatively small lattices) presumes that $D(0;L)$ vanishes in the thermodynamic limit ($c_1 = 0$).

We apply these four fit-formulas to $D^{\rm fc}(0;L)$, $D^{\rm bc}_{\rm SA}(0;L)$, and $D^{\rm bc}_{\rm FSA}(0;L)$. The comparison of different fits serves to check the stability of the results.

Fit-formulas (A), (B), and (C) provide a good fit of propagators with $\chi^2/n_{\rm df} \leq 1.4$. The best fit is provided by formula (B), fit (A) is only slightly worse, both of them give significantly smaller errors in the infinite-volume extrapolation than fit (C).

In all three cases [i.e., (A), (B), and (C)] the values of $D(0)$ in the thermodynamic limit *differ* from zero which is in agreement with the statement made in [14,18].

In contrast, the quality of the fit with fit-formula (D) in most cases is much worse (with $\chi^2/n_{\rm df}$ up to 15). Therefore, we exclude fit-formula (D) from the further consideration.

The infinite-volume values of $D^{\rm bc}_{\rm FSA}(0)$ obtained by fit-formulas (A), (B), and (C) coincide within 1–2 standard deviations for both values of β under consideration; the same is valid also for $D^{\rm bc}_{\rm SA}(0)$. The infinite-volume values of $D^{\rm fc}(0)$ obtained by fit-formulas (A), (B), and (C) coincide (within errorbars) only for $\beta = 10.21$, whereas for $\beta = 7.09$ they fall within 5 standard deviations. Such discrepancy can be due to significant finite-volume contributions of the order $1/L^2$ for small lattices.

We also checked the stability of the fit-parameters by excluding the lattice of minimum volume from consideration. Such an exclusion has a negligible effect on the fit-parameters.

In Fig. 1 we show our values of $D(0;L)$ calculated for $\beta = 7.09$ (left panel) and $\beta = 10.21$ (right panel) in the bc FSA, fc, and wc FSA cases. The lines represent fits according to fit-formula (A) (however, we note that in the wc case the fit is unstable).

Moreover, Fig. 1 demonstrates another interesting phenomenon: the Gribov copy influence remains rather strong even in the thermodynamic limit. Indeed, the infinite-volume extrapolation of $D^{\rm fc}(0)$ *differs* from infinite-volume extrapolation of $D^{\rm bc}(0)$. This difference is observed for all values of β and all fit formulas in agreement with our observation made in [18] for $\beta = 4.24$.

Therefore, the expectation values over the Gribov region Ω are *different* in the infrared from that calculated in the fundamental modular region Γ that disagrees with the statements made in [21]. This is the main result of our paper.

At the same time, as in [18] we found that while finite L $D^{\rm bc}_{\rm SA}(0,L)$ is higher than $D^{\rm bc}_{\rm FSA}(0,L)$, in the infinite volume they coincide within error bars. This remarkable agreement confirms the reliability of our estimation of $D(0)$ in the infinite-volume limit.

For better illustration of our main result, we calculated additionally the averaged difference between fc and bc propagators normalized to $D^{\rm bc}(p;L=\infty)$,

$$W(p) = \frac{D^{\rm fc}(p) - D^{\rm bc}(p)}{D^{\rm bc}(p;L=\infty)}. \tag{12}$$

In Fig. 2 we show the dependence of $W(0)$ on the inverse lattice size both for FSA and SA procedures. For FSA the value of $W(0)$ decreases for rising size, while for SA $W(0)$ it grows. To fit data for $W(0)$ we used fit formulas (A) and (B). The lines in Fig. 2 are for fit (B) since in this case it is much better than fit (A).

For smaller volumes the values of $W(0)$ for the SA procedure, $W_{\rm SA}(0)$, are close to zero ("Gribov noise"), while $W_{\rm FSA}(0)$ is at its maximum. The last observation corresponds to strong effects of flip sectors (see, e.g., [18]). However, with increasing volume, $W_{\rm SA}(0)$ is increasing, indicating the increasing role of the copies within a given flip sector. Conversely, decreasing of $W_{\rm FSA}(0)$ with increasing volume implies that the role of the flip sectors reduces.

Remarkably, in the limit $L \to \infty$, the values $W_{\rm FSA}(0)$ and $W_{\rm SA}(0)$ coincide (within error bars), which confirms the reliability of our fitting procedure. Results for both procedures imply *a nonzero* difference between fc and bc values of the propagators of ∼30–40% in the thermodynamic limit. Thus, the effect is very strong. Note that the asymptotic value $W(0, L=\infty)$ depends weakly (if at all) on the value of the spacing a.

In Fig. 3 we show the momentum dependence of $D^{\rm bc}_{\rm FSA}(p)$ for three different values of β (i.e., for three different values of spacing a). In all three cases the physical volumes are approximately equal with $aL \simeq 6.0$ fm. One can see that the finite-spacing effects are very small for large momenta and are still small (∼1–2%) for $|p| \lesssim 400$ MeV if data for $\beta = 7.09$ and $\beta = 10.21$ are compared. For larger values of $|p|$, finite-spacing effects are even much less. We conclude that (at least) for $\beta = 10.21$, we can speak about the propagator $D^{\rm bc}_{\rm FSA}(p)$ in the continuum limit.

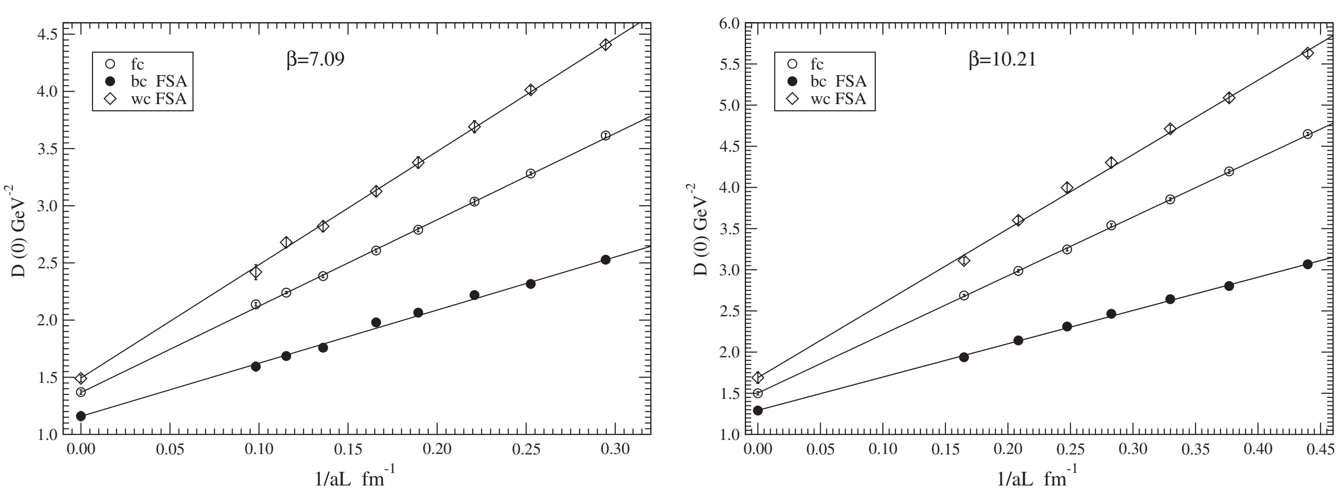

FIG. 1. $D(0)$ as a function of $1/aL$ for $\beta = 7.09$ (Left) and for $\beta = 10.21$ (Right). Lines show results of the fit to the function (A) (however, we note that in the wc case the fit is unstable).

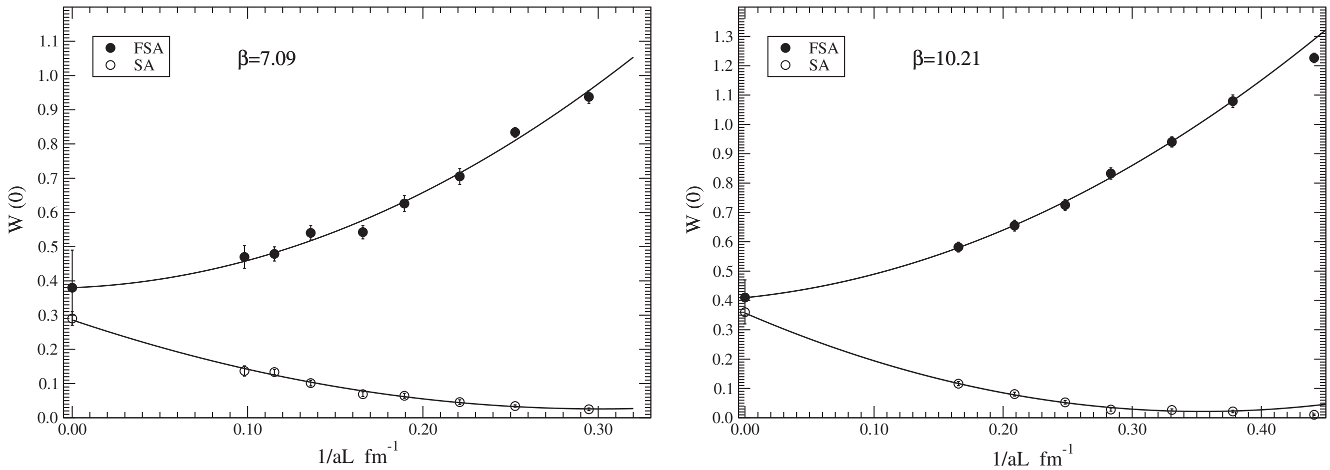

FIG. 2. $W(0)$ as a function of $1/aL$ for $\beta = 7.09$ (Left) and $\beta = 10.21$ (Right). Lines show results of the fit to the function (B).

Note that the propagator has a maximum at nonzero value of momentum $|p| \sim 400$ MeV. Therefore, the behavior of $D(p)$ in the deep infrared region is inconsistent with a simple pole-type dependence.

In Fig. 4 we compare the momentum dependence of the bc gluon propagator calculated for four different volumes for $\beta = 10.21$. Apart from $p = 0$ case, the finite-volume dependence can be seen for comparatively small values of momenta, i.e., $|p| \lesssim 0.5$ GeV. For larger values of momenta, the volume dependence quickly disappears.

To compare Gribov copy effects for different values of L and various momenta, we define the Gribov copy sensitivity parameter $\Delta(p) \equiv \Delta(p; L)$ as a normalized difference of the fc and bc gluon propagators,

$$\Delta(p) = \frac{D^{\mathrm{fc}}(p) - D^{\mathrm{bc}}_{\mathrm{FSA}}(p)}{D^{\mathrm{bc}}_{\mathrm{FSA}}(p)}, \tag{13}$$

where the numerator is the average of the differences between fc and bc propagators calculated for every configuration and normalized with the bc (averaged) propagator.

In Fig. 5 we show the momentum dependence of $\Delta(p)$. In the left panel $\Delta(p)$ for $\beta = 7.09$ for two volumes is depicted. As one can see, the Gribov copy influence is very strong in deep infrared. For a given value of L, the parameter $\Delta(p)$ decreases quickly with an increase of the momentum. One can also see that for a fixed nonzero physical momentum, $\Delta(p)$ tends to decrease with increasing L. These observations are in agreement with the observations made earlier in [18] and for the four-dimensional $SU(2)$ theory [32]. Quantitatively our results for $\beta = 7.09$ and $\beta = 10.21$ satisfy the following constraint: $\Delta(p) \lesssim 0.05$ for $pL \gtrsim 10$. In the right panel of Fig. 5 $\Delta(p)$ for two lattices ($L = 64$, $\beta = 7.09$ and $L = 96$, $\beta = 10.21$) with $aL \simeq 6$ fm are presented. The data indicate that $\Delta(p)$ does *not* decrease with decreasing a.

Figure 6 demonstrates the dependence of the zero-momentum propagators $D(0)$ on spacing a in the thermodynamic limit where the results of fit formula (B) were used for $L \to \infty$. As one can see, this dependence is rather weak

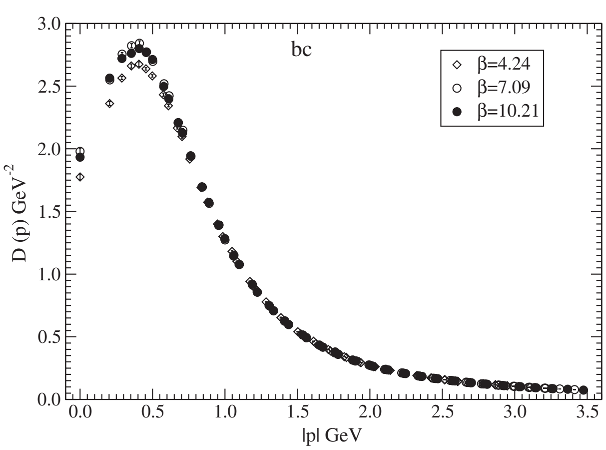

FIG. 3. $D^{\mathrm{bc}}_{\mathrm{FSA}}(p)$ as a function of $|p|$ for $\beta = 4.24$, $\beta = 7.09$ and $\beta = 10.21$. In all three cases $aL \simeq 6.0$ fm. Data for $\beta = 4.24$ are taken from [18].

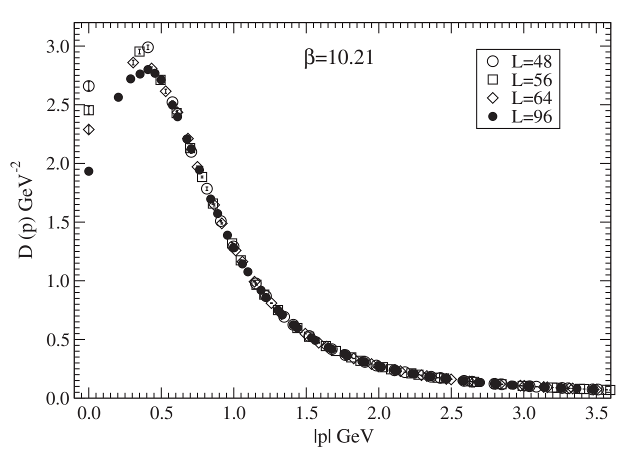

FIG. 4. Momentum dependence of $D^{\mathrm{bc}}_{\mathrm{FSA}}(p)$ for $\beta = 10.21$ and four different volumes.

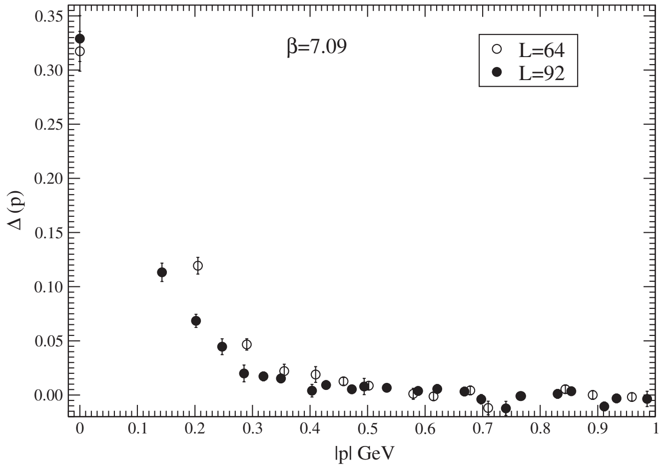

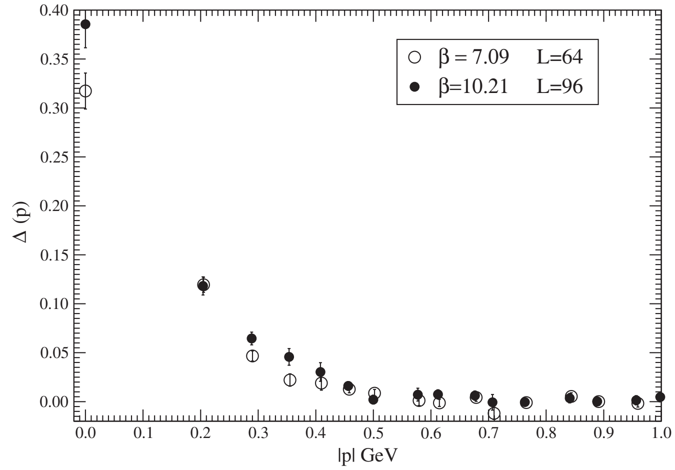

FIG. 5. $\Delta(p)$ as a function of p for two lattice sizes at $\beta = 7.09$ (left) and for approximately equal physical lattice sizes at $\beta = 7.09$ and 10.21 (right).

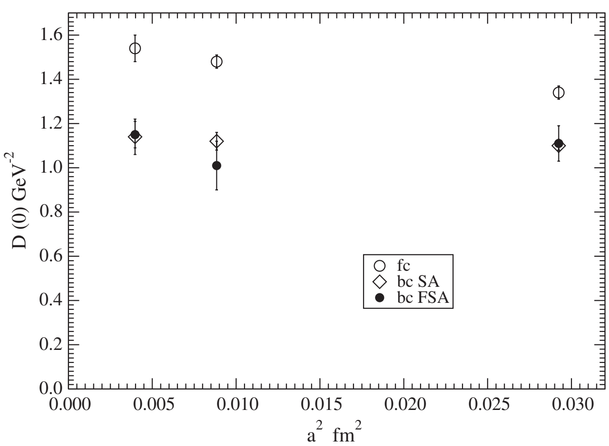

FIG. 6. $D(0)$ as a function of a^2 for $L \to \infty$.

when $a \to 0$, and the values obtained at $\beta = 10.21$ are very close to the respective continuum limit values. We should emphasize that our results for $p = 0$ for all lattice spacings (see also Fig. 1 and Fig. 2) as well as our results for small *nonzero* physical momentum presented in [18] imply that there are comparatively small nonzero momenta where Gribov copy effects also survive in the thermodynamic limit.

The last observation is essential also for the calculation of, e.g., screening masses in four-dimensional theory at nonzero temperature, where the momentum dependence of the gluon propagator $D(p)$ in the infrared region is important.

IV. CONCLUSIONS

We investigated numerically the Landau gauge gluon propagator $D(p)$ in the three-dimensional pure gauge $SU(2)$ lattice theory. We have employed lattices with various values of L for $\beta = 7.09$ ($a = 0.094$ fm) and $\beta = 10.21$ ($a = 0.063$ fm). This work is the continuation of our previous paper [18], where most calculations were done for $\beta = 4.24$ ($a = 0.17$ fm).

The main goal of this work was to confirm our observations made earlier in [18] employing larger values of β and to draw some definite conclusions about the continuum limit of the theory.

Special attention in this study has been paid to the dependence on the choice of Gribov copies. To this purpose we have generated up to 280 gauge copies for every configuration. Our bc FSA method provides systematically higher values of the gauge-fixing functional as compared to the fc and bc SA methods. We stress that the choice of the efficient gauge-fixing procedure is of crucial importance in the study of the gluon propagator in the Landau gauge.

Our main results are the following:

(1) The Gribov copy effects are very strong in the deep infrared region. Moreover, fc propagators do *not* coincide with the bc propagators even in the infinite-volume limit $L \to \infty$ (with difference up to ∼30÷40%). Therefore, the expectation values over the Gribov region Ω are *different* in the infrared from that calculated in the fundamental modular region, i.e.,

$$\langle O \rangle_\Omega \neq \langle O \rangle_\Gamma, \tag{14}$$

which does not confirm the statements made in [21].

(2) In the deep infrared the Gribov copy effects for $D(p)$ do *not* decrease with a decrease of the lattice spacing. So, we conclude that the difference between averaging over Gribov region Ω and fundamental modular region Γ persists also in the continuum limit.

(3) We find strong indications that in the thermodynamic limit $L \to \infty$ the value of $D(0; L)$ differs from zero. This is in agreement with the RGZ scenario and the decoupling solution of DSE, and confirms the results of numerical computations in Refs. [14,18].

With decreasing the lattice spacing a, the value of $D(0;\infty)$ does *not* show the tendency to decrease.

(4) Comparing results for $\beta = 10.21$ and $\beta = 7.09$, we find that the finite-spacing effects for $D^{\mathrm{bc}}_{\mathrm{FSA}}(p)$ appear to be rather small in the infrared and they are absent for large momenta (see Fig. 3 and Fig. 6). Thus the data obtained for $\beta = 10.21$ are a good approximation for the continuum limit.

ACKNOWLEDGMENTS

This investigation was partly supported by the Heisenberg-Landau program of collaboration between the Bogoliubov Laboratory of Theoretical Physics of the Joint Institute for Nuclear Research Dubna (Russia) and German institutes, by Grant No. RFBR 13-02-01387. V. B. is supported by Grant No. RFBR 11-02-01227-a.

[1] V. N. Gribov, Nucl. Phys. **B139**, 1 (1978).
[2] D. Zwanziger, Nucl. Phys. **B364**, 127 (1991).
[3] D. Dudal, S. P. Sorella, N. Vandersickel, and H. Verschelde, Phys. Rev. D **77**, 071501 (2008).
[4] D. Dudal, J. A. Gracey, S. P. Sorella, N. Vandersickel, and H. Verschelde, Phys. Rev. D **78**, 065047 (2008).
[5] D. Dudal, J. A. Gracey, S. P. Sorella, N. Vandersickel, and H. Verschelde, Phys. Rev. D **78**, 125012 (2008).
[6] L. von Smekal, R. Alkofer, and A. Hauck, Phys. Rev. Lett. **79**, 3591 (1997).
[7] R. Alkofer and L. von Smekal, Phys. Rep. **353**, 281 (2001).
[8] J. M. Cornwall, Phys. Rev. D **26**, 1453 (1982).
[9] C. S. Fischer, A. Maas, and J. M. Pawlowski, Ann. Phys. (Berlin) **324**, 2408 (2009).
[10] A. C. Aguilar, D. Binosi, and J. Papavassiliou, Phys. Rev. D **78**, 025010 (2008).
[11] P. Boucaud, J. P. Leroy, A. L. Yaouanc, J. Micheli, O. Pène, and J. Rodríguez-Quintero, J. High Energy Phys. 06 (2008) 012.
[12] A. Cucchieri, T. Mendes, and A. R. Taurines, Phys. Rev. D **67**, 091502 (2003).
[13] A. Cucchieri, T. Mendes, and A. R. Taurines, Phys. Rev. D **71**, 051902 (2005).
[14] A. Cucchieri and T. Mendes, *Proc. Sci.*, LAT2007 (**2007**) 297 [arXiv:0710.0412].
[15] A. Cucchieri, A. Maas, and T. Mendes, Phys. Rev. D **75**, 076003 (2007).
[16] A. Maas, Phys. Rev. D **79**, 014505 (2009).
[17] A. Cucchieri, D. Dudal, T. Mendes, and N. Vandersickel, Phys. Rev. D **85**, 094513 (2012).
[18] V. Bornyakov, V. Mitrjushkin, and R. Rogalyov, Phys. Rev. D **86**, 114503 (2012).
[19] A. Maas, Phys. Rep. **524**, 203 (2013).
[20] M. A. Semenov-Tyan-Shanskii and V. A. Franke, Zap. Nauchn. Semin. LOMI **120**, 159 (1982) [J. Sov. Math. **34**, 1999 (1986)].
[21] D. Zwanziger, Phys. Rev. D **69**, 016002 (2004).
[22] M. J. Teper, Phys. Rev. D **59**, 014512 (1998).
[23] J. E. Mandula and M. Ogilvie, Phys. Lett. B **185**, 127 (1987).
[24] C. Parrinello and G. Jona-Lasinio, Phys. Lett. B **251**, 175 (1990).
[25] D. Zwanziger, Nucl. Phys. **B345**, 461 (1990).
[26] A. Nakamura and M. Plewnia, Phys. Lett. B **255**, 274 (1991).
[27] V. G. Bornyakov, V. K. Mitrjushkin, M. Müller-Preussker, and F. Pahl, Phys. Lett. B **317**, 596 (1993).
[28] V. K. Mitrjushkin, Phys. Lett. B **389**, 713 (1996).
[29] I. L. Bogolubsky, G. Burgio, V. K. Mitrjushkin, and M. Müller-Preussker, Phys. Rev. D **74**, 034503 (2006).
[30] I. L. Bogolubsky, V. G. Bornyakov, G. Burgio, E.-M. Ilgenfritz, V. K. Mitrjushkin, and M. Müller-Preussker, Phys. Rev. D **77**, 014504 (2008).
[31] V. G. Bornyakov, V. K. Mitrjushkin, and M. Müller-Preussker, Phys. Rev. D **79**, 074504 (2009).
[32] V. Bornyakov, V. Mitrjushkin, and M. Muller-Preussker, Phys. Rev. D **81**, 054503 (2010).
[33] V. Bornyakov and V. Mitrjushkin, Phys. Rev. D **84**, 094503 (2011).
[34] V. Bornyakov and V. Mitrjushkin, Int. J. Mod. Phys. A **27**, 1250050 (2012).
[35] R. Aouane, V. G. Bornyakov, E.-M. Ilgenfritz, V. K. Mitrjushkin, M. Müller-Preussker, and A. Sternbeck, Phys. Rev. D **85**, 034501 (2012).
[36] L. von Smekal, A. Jorkowski, D. Mehta, and A. Sternbeck, *Proc. Sci.*, Confinement 8 (**2008**) 048 [arXiv:0812.2992].
[37] A. Sternbeck and M. Müller-Preussker, *Proc. Sci.*, Confinement X (**2013**) 074 [arXiv:1304.1416].
[38] C. Hughes, D. Mehta, and J.-I. Skullerud, Ann. Phys. (Berlin) **331**, 188 (2013).
[39] P. Schemel, Diplom thesis, Humboldt University, Berlin, 2006.
[40] I. L. Bogolubsky, V. G. Bornyakov, G. Burgio, E.-M. Ilgenfritz, M. Müller-Preussker, P. Schemel, and V. K. Mitrjushkin, *Proc. Sci.*, LAT2007 (**2007**) 318 [arXiv:0710.3234].